European Journal of Radiology 83 (2014) 1771–1777

Contents lists available at ScienceDirect

European Journal of Radiology

journal homepage: www.elsevier.com/locate/ejrad

Image and pathological changes after microwave ablation of breast cancer: A pilot study

Wenbin Zhou[a,1], Yanni Jiang[b,1], Lin Chen[a], Lijun Ling[a], Mengdi Liang[a], Hong Pan[a], Siqi Wang[b], Qiang Ding[a], Xiaoan Liu[a,*], Shui Wang[a,**]

[a] Department of Breast Surgery, The First Affiliated Hospital, Nanjing Medical University, 300 Guangzhou Road, Nanjing 210029, China
[b] Department of Radiology, The First Affiliated Hospital, Nanjing Medical University, 300 Guangzhou Road, Nanjing 210029, China

ARTICLE INFO

Article history:
Received 24 April 2014
Received in revised form 14 June 2014
Accepted 20 June 2014

Keywords:
Breast cancer
Microwave ablation
MR imaging

ABSTRACT

Purpose: To prospectively assess MR imaging evaluation of the ablation zone and pathological changes after microwave ablation (MWA) in breast cancer.
Materials and methods: Twelve enrolled patients, diagnosed with non-operable locally advanced breast cancer (LABC), were treated by MWA and then neoadjuvant chemotherapy, followed by surgery. MR imaging was applied to evaluate the effect of MWA. Hematoxylin-eosin (HE) staining and transmission electron microscopy (TEM) were applied to analyze the ablated area.
Results: All MWA procedures were performed successfully under local anesthesia. For a mean duration of 2.15 min, the mean largest, middle and smallest diameters in the ablated zone 24-h post-ablation in MR imaging were 2.98 cm ± 0.53, 2.51 cm ± 0.41 and 2.23 cm ± 0.41, respectively. The general shape of the ablation zone was close to a sphere. The ablated area became gradually smaller in MR imaging. No adverse effects related to MWA were noted in all 12 patients during and after MWA. HE staining could confirm the effect about 3 months after MWA, which was confirmed by TEM.
Conclusions: 2 min MWA can cause an ablation zone with three diameters larger than 2 cm in breast cancer, which may be suitable for the local treatment of breast cancer up to 2 cm in largest diameter. However, the long-term effect of MWA in the treatment of small breast cancer should be determined in the future.

1. Introduction

Image-guided nonsurgical ablative therapies, including radiofrequency, microwave, cryotherapy and laser therapy, have received increasing attention as minimally invasive treatments to destroy various solid tumors [1–4]. Microwave ablation (MWA) is a promising minimally invasive local therapy with many advantages [5–7], including large ablation zones, short ablation durations, and improved convection profile. MWA has been accepted as an effective therapy in the treatment of hepatic tumors [8–10], and has been applied to treat other solitary tumors [11–14].

Since satisfied cosmetic outcomes may be obtained by nonsurgical ablative therapies without the removal of breast tissue, ablative therapies have been evaluated in many clinical research studies [3,15–18]. Our previous phase I ablation-resection study firstly shows that MWA of small breast cancers is feasible under general anesthesia, but the extent of ablation zone may be underestimated [11]. To our knowledge, there is no study reporting the long-term evolution of microwave ablated breast cancer. For clinical use of MWA for breast cancer, the long-term evolution of ablated lesions is urgently needed.

MR imaging can be used to predict tissue damage after ablation because necrosis is typically visualized as a nonperfused volume after contrast material administration [19,20]. So it is suitable for evaluating the efficacy of MWA. Previous studies suggest MR imaging is suitable for long-term follow-up of radiofrequency ablated breast cancer [17,20]. The pathological confirmation of the efficacy is the gold standard for MWA of breast cancer. The pathological findings are only reported in few studies about radiofrequency ablation of breast cancer [15,16]. Moreover, the correlation between MR imaging and pathological findings is necessary for long-term follow-up. Up to now, the correlation is only reported in a previous study about radiofrequency [16].

* Corresponding author. Tel.: +86 25 83718836x8621; fax: +86 25 83718836.
** Corresponding author. Tel.: +86 25 83718836x6456; fax: +86 25 83718836.
E-mail addresses: liuxiaoan@126.com (X. Liu), ws0801@hotmail.com (S. Wang).
[1] These authors contributed equally to this work.

http://dx.doi.org/10.1016/j.ejrad.2014.06.015
0720-048X/

MWA has not been applied for local therapy for breast cancer patients. MR imaging and pathological changes after microwave ablation of breast cancer have not been reported. In this prospective study, we report the data about MR imaging evaluation of the ablation zone and pathological changes after MWA in breast cancer for the first time.

2. Materials and methods

2.1. Patient enrollment

The study protocol was approved by the institutional ethics committee (No. 2011-SR-106), and written informed consent was provided by all patients. From February 2012 to September 2013, patients diagnosed with LABC in our hospital were recruited in this prospective pilot study.

The inclusion criterion were as follows: (a) invasive breast cancer proved by using core-needle biopsy; (b) non-operable LABC; (c) patients who wanted to receive neoadjuvant chemotherapy; and (d) Karnofsky performance status greater than 70% [11,18]. Patient exclusion criteria included the following: (a) patients not suitable for neoadjuvant chemotherapy; (b) patients with medical contraindications to MR imaging; (c) patients with evidence of coagulopathy, chronic liver diseases, or renal failure; (d) patients taking anticoagulant drugs; and (e) patients who were pregnant or breast-feeding. Hormone receptor and human epidermal growth factor receptor 2 status were determined by using immunohistochemical analysis of tissue from core-needle biopsy specimens prior to treatment.

2.2. Treatment procedure

Breast MR imaging was performed before treatment by two radiologists with more than 1500 interpretations experience in breast MR imaging. Then, MWA was performed by two surgeons with 17 and 5 years of experience in breast surgery, respectively. Second breast MR imaging evaluation was performed about 24 h after MWA. Patients received prescheduled neoadjuvant chemotherapy after second MR imaging evaluation. Breast MR imaging was performed before every subsequent cycle of neoadjuvant chemotherapy and surgery. Modified radical mastectomy (mastectomy and axillary lymph node dissection) was scheduled to these patients when the disease became operable. Patients were monitored during the MWA, the following chemotherapy and surgery for any MWA-induced complications by the surgeons and radiologists.

2.3. MWA protocols

The patient was placed in the supine position. Ultrasonography (US) was applied to guide MWA. Local anesthesia was induced with 1% lidocaine. Lidocaine was injected around the lesion and into retromammary space. With US guidance, the antenna was placed into the tumor. MWA was started for 2–3 min after testing the cold-water cycling system. When the patient could not tolerate the pain, the procedure was interrupted. The microwave system used in this study was the same as previous studies [7,11]. The microwave irradiation frequency was 2450 MHz, and an output power of 40 W was chosen. After ablation, patients were monitored in our hospital for at least 24 h for immediate complications.

2.4. Neoadjuvant chemotherapy

Patients received at least three 21-day cycles of neoadjuvant chemotherapy before surgery. Chemotherapy regimens were determined based on guidelines in our country and included: (1) TEC: docetaxel, epirubicin, and cyclophosphamide; (2) FEC: 5-fluorouracil, epirubicin, and cyclophosphamide; (3) NP: navelbine and cisplatin; (4) TP: docetaxel and cisplatin. After two cycles of neoadjuvant chemotherapy, clinical response was assessed by physical examination or US. When the disease progressed, the primary regimen was replaced by a new regimen.

2.5. MR imaging protocols

MR imaging was performed with a 3.0 T system (MAGNETOM Trio, Siemens, Germany) using a bilateral 8 channel phased-array breast coil with women in the prone position. Axial and sagittal T1-weighted and T2-weighted images were obtained.

The dynamic series consisted of a three-dimensional transverse fast low angle shot T1-weighted sequence (TR/TE, 4.23 ms/1.57 ms; matrix 448×296; slice thickness 0.9 mm, no gap; pixel resolution 1.1 mm $\times$ 0.8 $\times$ mm 0.9 mm) with fat suppression. A total of six dynamic acquisitions, with a temporal resolution of 60 s for a single dynamic acquisition, were performed. Contrast agent bolus injection consisted of 0.1 mmol gadopentetate dimeglumine (Magnevist, BayerSchering, Germany) per kilogram of body weight was administered at an injection rate of 3.0 ml/s, which was followed by a 20 ml saline solution.

The ablated tumor was defined as a nonperfused volume after contrast material administration [19,20]. Ablation extent was calculated on a voxel-by-voxel basis. The projections were made in the axial, sagittal and coronal directions and allowed the ablation zone to be identified in all dimensions. Two diameters in largest cross section and the largest height in coronal plane of ablated volumes in MR imaging were defined as largest, middle, and smallest diameters according to their length. The shapes of the ablated volumes were classified according to the ellipticity index calculated by using largest, middle, and smallest diameters in MR imaging. Accordingly, the fraction of the largest and smallest diameters was defined as Dl, and the fraction of the middle and smallest diameters was defined as Dm [16]. According to the previous study [16], a lesion was called spherical when both Dl and Dm were 1.5 or less.

2.6. Pathologic evaluation

After surgery, the coagulation zones were dissected and sectioned along the antenna track. The tissue sections were incubated for cell viability in the incubation medium with 2% 2,3,5-triphenyl tetrazolium chloride (Sigma) [7,21]. The largest diameter (along the antenna) was assessed macroscopically with calipers. After incubation, the tissues were fixed in formalin, embedded in paraffin, sectioned into 4-μm slices and stained with hematoxylin-eosin (HE). The pathology evaluation was performed by two pathologists (with more than 10 years of experience in breast pathologic examination).

Ultrastructure analyses with transmission electron microscopy (TEM) of the ablative zone and normal zone were performed. The ablative samples were collected from the center of the ablative zone, while the normal ones from peripheral normal breast tissues at least 3 cm away from the ablative zone. The electron microscope samples were prepared according to the guidelines. Ultrathin sections (50–80 nm) were cut and examined and micrographed with a transmission electron microscope (JEM-1010, Japan).

2.7. Data and statistical analysis

Mean $\pm$ standard deviation (SD), percentiles, and range were analyzed for each continuous variable. The volume of coagulation was calculated by using the three-dimensional axis in MR imaging with the equation $V = 4\pi(a/2)(b/2)(c/2)/3$. The association between the largest diameter in pathology and MR imaging was evaluated

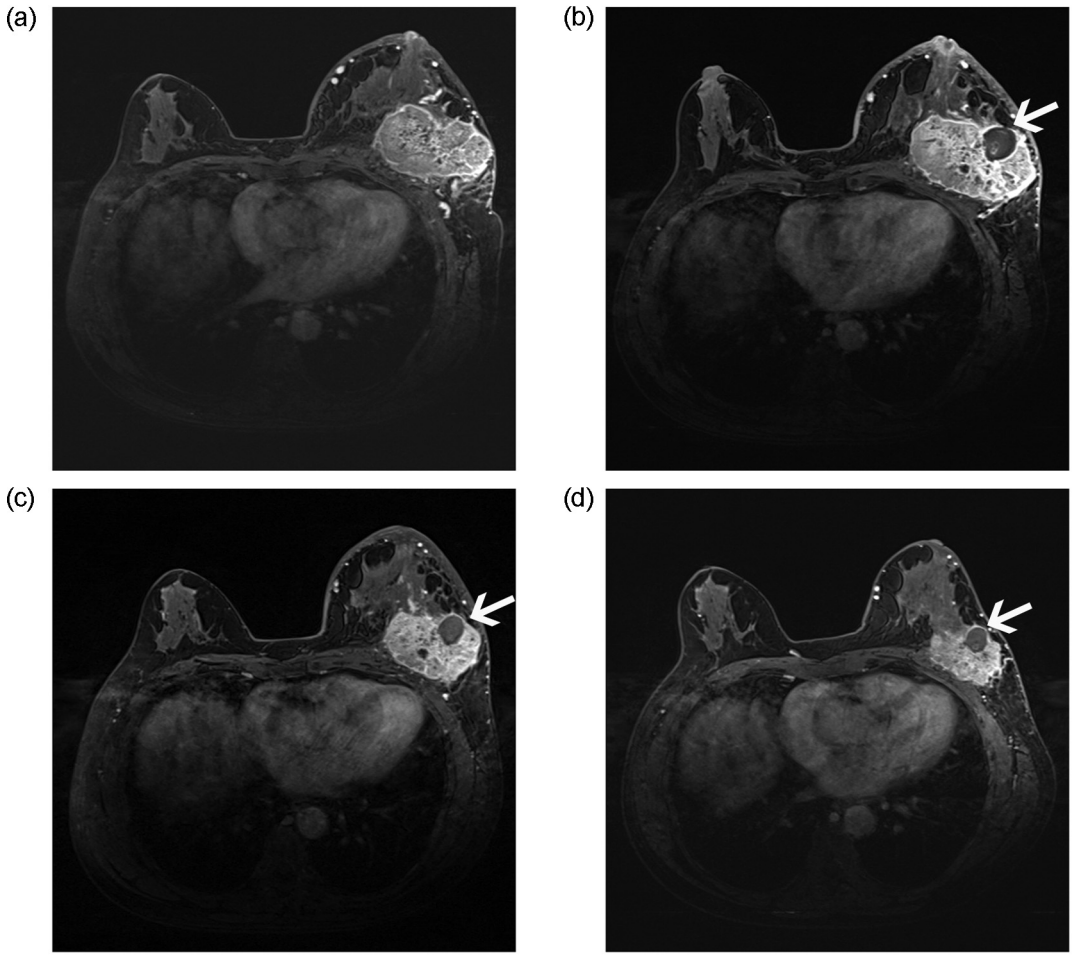

Fig. 1. MR images acquired by the three-dimensional transverse fast low angle shot. T1-weighted sequence with fat suppression in 58-year-old woman shows the evolution of ablated breast cancer. (a) MR image before treatment. (b) MR images 24-h post-ablation shows the ablated zone (arrow) without enhancement. The margin is clear and smooth. (c) MR image 3-week post-ablation shows the ablated zone (arrow) is still clear and the diameters significantly decrease. (d) MR image before surgery shows a gradual decrease of the diameters of the ablated zone (arrow).

by using Spearman rank correlation. All *P*-values were two-tailed with 5% significance levels. All statistical analyses were performed by using software STATA version 11.0 (Computer Resource Center, America).

3. Results

3.1. Baseline characteristics

Twelve patients were enrolled. The median patient age was 54 years (range, 34–61 years). Of these 12 patients, ten were diagnosed with invasive ductal carcinoma, one was diagnosed with invasive lobular carcinoma, and the other one was diagnosed with sarcomatoid carcinoma. Besides, six were diagnosed with hormone receptor negative breast cancer, and three were human epidermal growth factor receptor 2 overexpression. Of these 12 patients, one had been treated with one cycle of TEC regimen, and another one had been treated with two cycles of FEC regimen in other institutions before treatment in our hospital. All patients were diagnosed with non-operable LABC with a largest diameter > 5 cm by physical examination and MR imaging in our hospital.

3.2. MWA procedure

Of these 12 patients, MWA procedures were performed successfully under local anesthesia. However, two patients suffered from obvious pain, and the procedure was interrupted. Therefore, the two patients were ablated for 80 s and 90 s, respectively. The other ten patients tolerated the procedure well. Of the 10 patients, seven were ablated for 2 min, and the other three ablated for 3 min The mean ablation time was 2.15 min, ranging from 1.3 to 3 min

3.3. Features of ablation zone in MR imaging

Characteristics of ablation zone in dynamic scan: MR images revealed a zone of ablation without enhancement about 24-h after MWA. In 3 cases, there was a small amount of bleeding in ablation zone 24-h after MWA, while in the other 9 cases, there was no bleeding. Among the subsequent series of MR examinations of ablation zone, there was no bleeding in all cases. The margin of ablation zone was clear and smooth in all cases.

Size, shape and evolution of ablation zone in MR imaging: MR imaging was used to evaluate the ablated zone in three dimension about 24-h after MWA (Fig. 1). The mean largest diameter in the ablated zone was 2.98 ± 0.53 cm (range, 2.1–4.0 cm). The mean middle and smallest diameter were 2.51 ± 0.41 cm (range, 1.8–3.2 cm) and 2.23 ± 0.41 cm (range, 1.4–2.8 cm), respectively. Of seven patients ablated for 2 min, the three diameters were 3.06 ± 0.60 cm, 2.59 ± 0.40 cm and 2.30 ± 0.47 cm, respectively. The detailed information of ablation lesion according to ablation time was shown in Table 1. Since both Dl (mean, 1.35; range, 1.11–1.50) and Dm (mean, 1.13; range, 1.00–1.36) were not larger than 1.5 in

Table 1
Ablation lesion diameters and volumes according to ablation time.

Ablation time (n)	Largest diameter (cm)	Middle diameter (cm)	Smallest diameter (cm)	Ablated volume (cm^3)
All (12)	2.98 ± 0.53	2.51 ± 0.41	2.23 ± 0.41	9.31 ± 4.00
<2 min (2)	2.4 ± 0.14	2.0 ± 0.28	1.8 ± 0.14	4.52 ± 0.72
2 min (7)	3.06 ± 0.60	2.59 ± 0.40	2.30 ± 0.47	10.15 ± 4.42
3 min (3)	3.20	2.67 ± 0.31	2.37 ± 0.12	10.57 ± 1.19

all 12 cases, the general shape of the ablation zone was close to a sphere.

Importantly, MR imaging was also applied to evaluate the evolution of the ablated zone in 11 patients because one patient was lost. The ablated area detected by MR became gradually smaller (Fig. 1). The mean largest diameter of ablated zone significantly decreased from 2.89 ± 0.44 to 2.42 ± 0.35 cm ($P < 0.001$) about three weeks after MWA, and to 2.15 ± 0.34 cm before surgery (Fig. 2). The mean volume significantly decreased from 8.67 ± 3.48 to 5.20 ± 1.88 cm^3 ($P = 0.001$) about three weeks after MWA and to 3.60 ± 1.42 cm^3 before surgery (Fig. 2).

3.4. Histologic findings

In gross specimens (Fig. 3), a firm whitish ablated zone was readily apparent, and the antenna track could be found in the center of the ablated zone. The margin between the ablated zone and viable tissue was clear in all cases. However, the red hemorrhagic border surrounding the ablated zone was observed in only one case. No charring was observed in any case. 2,3,5-Triphenyl tetrazolium chloride staining confirmed that no viable cells were found in the ablated zone (Fig. 3).

HE staining (Fig. 4) revealed that the ablated tumor was replaced by the hyalinized and edematous stroma after MWA, and the outlines of cells seemed to still exist. The surrounding tumor showed decreased cellularity of cancer cells with hyalinized stroma after neoadjuvant chemotherapy. The border of the ablated zone was very clear.

The ablated area in TEM (Fig. 5) showed vague outlines of cells, and no intracytoplasmic mitochondria, endoplasmic reticulum and other organelles were observed. Cytoplasm was filled with granules of varying sizes and a small amount of vacuoles. Nuclear membrane ruptured and was partially lost. However, the surrounding cells showed clear cell membrane and integrated nucleus. Moreover, organelles, such as mitochondria and rough endoplasmic reticulum, were clearly visible.

Data of both MR imaging before surgery and 2,3,5-triphenyl tetrazolium chloride staining were available in eight cases. The Spearman correlation test showed good correlation between MR imaging and histologically determined ablation diameter in the largest axis ($r = 0.871$; 95% confidence interval: 0.49, 0.97; $P = 0.002$) (Fig. 6).

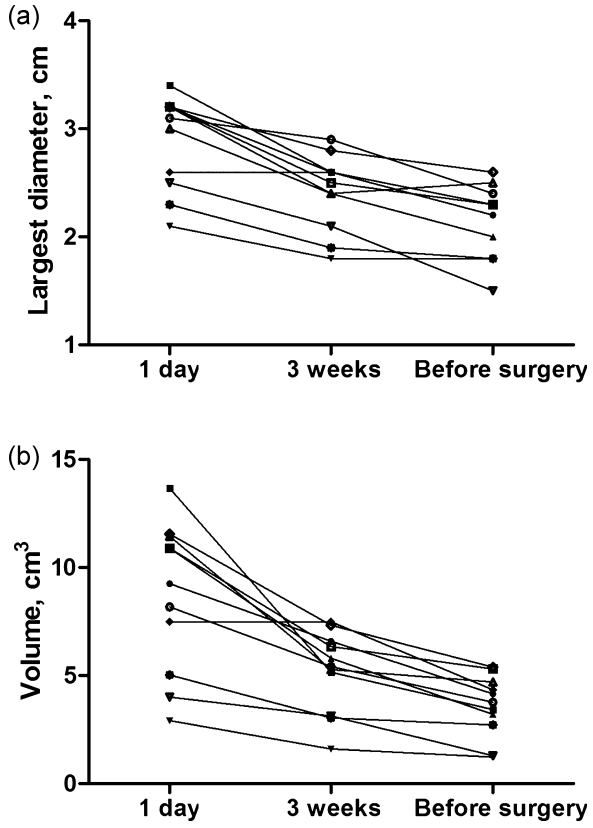

Fig. 2. The change of the largest diameter (a) and volume (b) of ablated zone 24-h post-ablation, 3-week post-ablation and before surgery in 11 patients. The mean largest diameter of ablated zone 24-h post-ablation significantly decreases from 2.89 ± 0.44 to 2.42 ± 0.35 cm about 3-week post-ablation, and to 2.15 ± 0.34 cm before surgery. The mean volume significantly decreases from 8.67 ± 3.48 to 5.20 ± 1.88 cm^3 about 3-week post-ablation and to 3.60 ± 1.42 cm^3 before surgery.

3.5. Adverse events

Of these 12 patients, 11 received prescheduled chemotherapy and surgery, and the other one was lost during the follow-up. In these 12 patients, no epidermal burn was observed. Of 11 patients receiving surgery, no thermal injury to the pectoralis major muscle was observed. In addition, no other adverse effects related to MWA were noted in all 12 patients during and after MWA.

4. Discussion

We firstly report successful experience of MWA in breast cancer under local anesthesia. Ten of all 12 patients tolerated MWA well. The three diameters of ablated zone were all larger than 2.3 cm about 24-h after MWA for 2 min, and the general shape was close to a sphere. Our results suggest MWA for 2 min may be enough for the local treatment of breast cancer up to 2 cm in largest diameter with a safety margin. Moreover, the ablated area detected by MR became gradually smaller. HE staining can confirm the effect about 3 months after MWA, which was confirmed by TEM.

The current study firstly reports the experience of MWA in the treatment of breast cancer under local anesthesia rather than under general anesthesia. Performance of MWA under local anesthesia more likely reflects the manner in which this modality could be utilized in the future [15]. Two patients experienced obvious pain, and they can still tolerate the pain. To avoid possible adverse effects, the procedure was interrupted. In the future, we suggest more lidocaine should be injected into retromammary space. Moreover, no skin burns or injury to pectoralis major muscle were observed, and the cosmesis was excellent in the current study. Our results support the use of MWA in the treatment of breast cancer.

Up to now, MWA has seldom been applied in the treatment of small breast cancer. MWA can ablate a large volume of breast cancer for a short duration [11]. The previous clinical study [11]

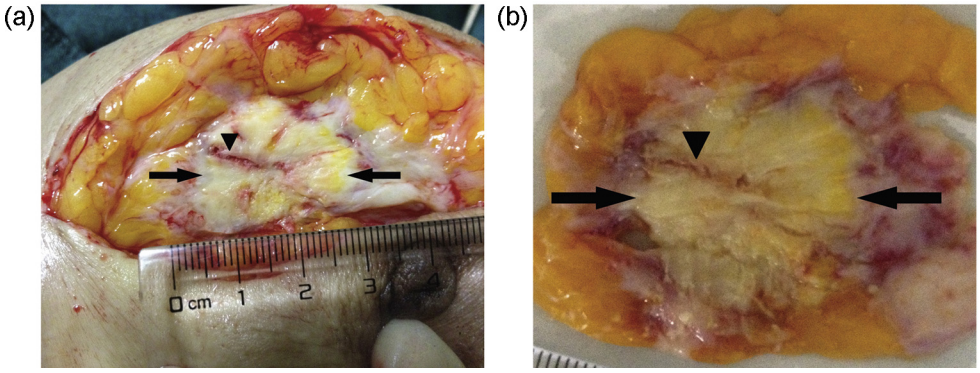

Fig. 3. Macroscopic appearances of excised specimen after surgery. (a) The ablated area (arrow), a firm whitish ablated zone, is readily apparent, and the antenna track (arrowhead) can be clearly identified in the center of the ablated zone. The margin between the ablated zone and viable tissue is clear. (b) 2,3,5-Triphenyl tetrazolium chloride staining of the specimen. The ablated area (arrow) is still white, while the surrounding viable tissue is stained with red. (For interpretation of the references to color in this figure legend, the reader is referred to the web version of this article.)

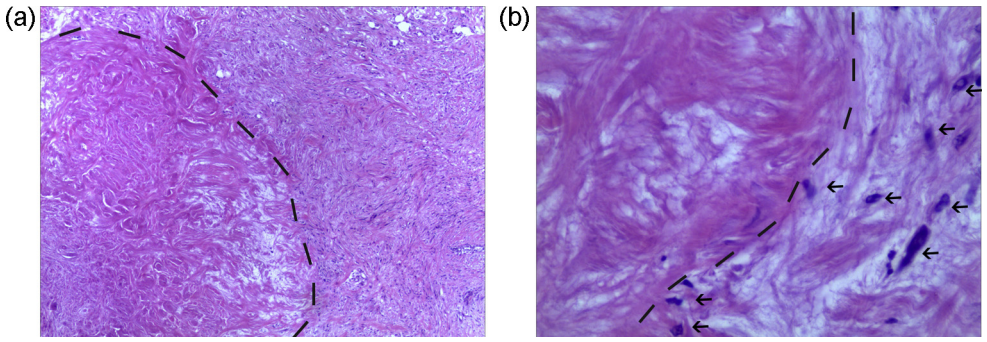

Fig. 4. HE staining (a, 4×; b, 40×) of ablative area and surrounding tissue shows clear border of the ablation zone. The ablated tumor (area at left) is replaced by the hyalinized and edematous stroma, while the surrounding tumor shows decreased cellularity of cancer cells (arrows) with hyalinized stroma after chemotherapy. The border (dashed line) of the ablated zone was very clear.

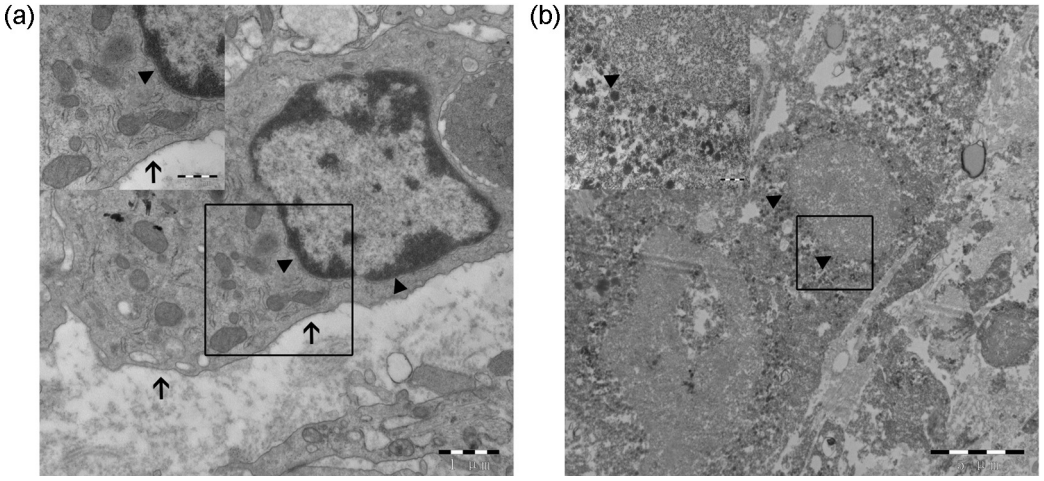

Fig. 5. Ultrastructures of the normal tissue (a) and ablative tumor (b) in TEM. (a) The surrounding cells show clear cell membrane (arrow) and integrated nucleus (arrowhead). Moreover, organelles were clearly visible. (b) The ablated area shows vague outlines of cells, and no organelles were observed. Cytoplasm was filled with granules of varying sizes and a small amount of vacuoles. Nuclear membrane (arrowhead) ruptured and was partially lost.

suggests that the coagulation zone with an average largest diameter of 2.77 cm can be achieved by MWA for 4.5 min. Furthermore, the ex vivo study [7] suggests the coagulation zone with an average largest diameter of about 2.80 cm can be achieved for 3 min. However, ablation zones in previous ablation-resection studies are underestimated. In the current study, the ablation zone was evaluated by MR imaging about 24 h after ablation according to a previous clinical study [22]. Wu and colleagues [23] found that the radiofrequency damaged zone increased rapidly within 2 h after ablation (about 95%), and then slowly reached the maximum on day 2. So our results accurately showed the maximum ablation zone in breast cancer. In this study, the ablation zone with an average largest diameter of about 3.0 cm can be achieved for about 2 min. Interestingly, the other two diameters were all larger than 2.30 cm, and the shape of the ablation zone was close to a sphere. Besides, chemotherapy was given to patients after MR evaluation, so the ablation zone did not

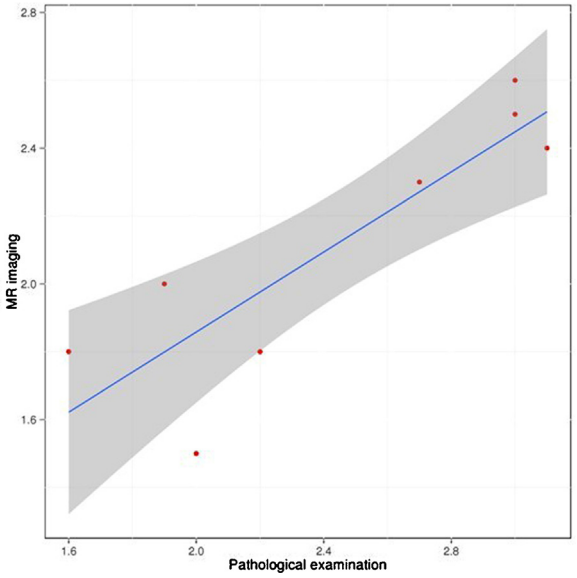

Fig. 6. Graph shows correlation between the largest diameter in pathology and MR imaging. A good correlation between the two variables is observed ($P = 0.002$).

increase by possible synergistic effect. Previous studies [7,24,25] suggest that the extent of ablation zone in MWA may be not affected by tissue heterogeneity. For complete ablation of breast cancer up to 2 cm in largest diameter with a safety margin, MWA for 2 min may be feasible with accurate position of the antenna.

Similarly to previous studies [16,17,26], MR imaging clearly demonstrated the ablation area without enhancement in all patients, and it correlated well with histological finding. Moreover, the margin of the ablation zone was clear and smooth in all cases. MR imaging, the most appropriate imaging technique for breast cancer [20,27], should be applied to evaluate the effect of MWA in the treatment of breast cancer. The present study firstly showed a long follow-up of MWA without resection. The ablated area detected by MR imaging after MWA became smaller as time passed. The ablated lesions shrank obviously in the first month after MWA, and then the lesions shrank slower than before. As previously described [26], the speed of shrinkage was slower than that expected, because the blood-flow of the breast is low. Future clinical studies should be taken to evaluate the resorption of microwave ablated breast cancer for a long-term follow-up.

In this study, HE staining could judge the tumor cell death in all cases about 3 months after MWA, and 2,3,5-triphenyl tetrazolium chloride staining confirmed that no viable cells were found in the ablated zone. However, this phenomenon was not observed in all cases after radiofrequency ablation (RFA) [26]. Furthermore, HE staining was confirmed by TEM in this study. The cell nucleus disintegrated completely. We infer that high energy of MWA may contribute to the difference. Moreover, the border of the ablated zone was very clear. HE staining could confirm the effect about 3 months after MWA.

Our previous study has found that slight thermal injuries to the skin and pectoralis major muscle were observed in three cases [11]. In this study, no skin burns were observed in these 12 patients. All these results suggest that MWA of breast cancer is safe.

Several limitations existed. First, the sample size was small, and our results should be confirmed by the future clinical trials. Second, most patients tolerated well under local anesthesia; some measures should be taken to improve the tolerance of MWA in the treatment of breast cancer. Third, this study showed accurate ablation zone in breast cancer; however, this study was performed in the neoadjuvant setting. The long-term effect of MWA in the treatment of small breast cancer should be determined in the future.

5. Conclusions

In conclusion, our results suggest 2 min MWA can cause an ablation zone with three diameters larger than 2.3 cm in breast cancer, which may be suitable for the local treatment of breast cancer up to 2 cm in largest diameter. Future clinical trials should be taken to determine the long-term effect of MWA in breast cancer.

Funding information

This work was supported in part by the National Natural Science Foundation of China (81270952, 81172505, 81202077 and 81272916), the Natural Science Foundation of Jiangsu Province (BK20141023), the Program for Development of Innovative Research Team in the First Affiliated Hospital of NJMU (IRT-008) and a project Funded by the Priority Academic Program Development of Jiangsu higher Education Institutions (PAPD).

Conflict of interest

All authors declare that they have no conflict of interest.

References

[1] Mirza AN, Fornage BD, Sneige N, Kuerer HM, Newman LA, Ames FC, et al. Radiofrequency ablation of solid tumors. Cancer J 2001;7:95–102.
[2] Morikawa S, Naka S, Murakami K, Kurumi Y, Shiomi H, Tani T, et al. Preliminary clinical experiences of a motorized manipulator for magnetic resonance image-guided microwave coagulation therapy of liver tumors. Am J Surg 2009;198:340–7.
[3] Sabel MS, Kaufman CS, Whitworth P, Chang H, Stocks LH, Simmons R, et al. Cryoablation of early-stage breast cancer: work-in-progress report of a multi-institutional trial. Ann Surg Oncol 2004;11:542–9.
[4] Amin Z, Donald JJ, Masters A, Kant R, Steger AC, Bown SG, et al. Hepatic metastases: interstitial laser photocoagulation with real-time US monitoring and dynamic CT evaluation of treatment. Radiology 1993;187:339–47.
[5] Simon CJ, Dupuy DE, Mayo-Smith WW. Microwave ablation: principles and applications. Radiographics 2005;25(Suppl. 1):S69–83.
[6] Yu J, Liang P, Yu X, Liu F, Chen L, Wang Y. A comparison of microwave ablation and bipolar radiofrequency ablation both with an internally cooled probe: results in ex vivo and in vivo porcine livers. Eur J Radiol 2011;79:124–30.
[7] Zhou W, Liang M, Pan H, Liu X, Jiang Y, Wang Y, et al. Comparison of ablation zones among different tissues using 2450-MHz cooled-shaft microwave antenna: results in ex vivo porcine models. PLoS One 2013;8:e71873.
[8] Liang P, Dong B, Yu X, Yu D, Wang Y, Feng L, et al. Prognostic factors for survival in patients with hepatocellular carcinoma after percutaneous microwave ablation. Radiology 2005;235:299–307.
[9] Lu MD, Chen JW, Xie XY, Liu L, Huang XQ, Liang LJ, et al. Hepatocellular carcinoma: US-guided percutaneous microwave coagulation therapy. Radiology 2001;221:167–72.
[10] Ong SL, Gravante G, Metcalfe MS, Strickland AD, Dennison AR, Lloyd DM. Efficacy and safety of microwave ablation for primary and secondary liver malignancies: a systematic review. Eur J Gastroenterol Hepatol 2009;21:599–605.
[11] Zhou W, Zha X, Liu X, Ding Q, Chen L, Ni Y, et al. US-guided percutaneous microwave coagulation of small breast cancers: a clinical study. Radiology 2012;263:364–73.
[12] Wang Y, Liang P, Yu X, Cheng Z, Yu J, Dong J. Ultrasound-guided percutaneous microwave ablation of adrenal metastasis: preliminary results. Int J Hyperthermia 2009;25:455–61.
[13] Wolf FJ, Grand DJ, Machan JT, Dipetrillo TA, Mayo-Smith WW, Dupuy DE. Microwave ablation of lung malignancies: effectiveness, CT findings, and safety in 50 patients. Radiology 2008;247:871–9.
[14] Vogl TJ, Naguib NN, Gruber-Rouh T, Koitka K, Lehnert T, Nour-Eldin NE. Microwave ablation therapy: clinical utility in treatment of pulmonary metastases. Radiology 2011;261:643–51.
[15] Burak Jr WE, Agnese DM, Povoski SP, Yanssens TL, Bloom KJ, Wakely PE, et al. Radiofrequency ablation of invasive breast carcinoma followed by delayed surgical excision. Cancer 2003;98:1369–76.
[16] Manenti G, Bolacchi F, Perretta T, Cossu E, Pistolese CA, Buonomo OC, et al. Small breast cancers: in vivo percutaneous US-guided radiofrequency ablation with dedicated cool-tip radiofrequency system. Radiology 2009;251:339–46.
[17] Palussiere J, Henriques C, Mauriac L, Asad-Syed M, Valentin F, Brouste V, et al. Radiofrequency ablation as a substitute for surgery in elderly patients with

nonresected breast cancer: pilot study with long-term outcomes. Radiology 2012;264:597–605.
[18] Vargas HI, Dooley WC, Gardner RA, Gonzalez KD, Venegas R, Heywang-Kobrunner SH, et al. Focused microwave phased array thermotherapy for ablation of early-stage breast cancer: results of thermal dose escalation. Ann Surg Oncol 2004;11:139–46.
[19] van den Bosch M, Daniel B, Rieke V, Butts-Pauly K, Kermit E, Jeffrey S. MRI-guided radiofrequency ablation of breast cancer: preliminary clinical experience. J Magn Reson Imaging 2008;27:204–8.
[20] Merckel LG, van den Bosch MA. Imaging-guided breast cancer ablation. Radiology 2012;265:322–3, author reply 323.
[21] Hines-Peralta AU, Pirani N, Clegg P, Cronin N, Ryan TP, Liu Z, et al. Microwave ablation: results with a 2.45-GHz applicator in ex vivo bovine and in vivo porcine liver. Radiology 2006;239:94–102.
[22] Lencioni R, Crocetti L, Petruzzi P, Vignali C, Bozzi E, Della Pina C, et al. Doxorubicin-eluting bead-enhanced radiofrequency ablation of hepatocellular carcinoma: a pilot clinical study. J Hepatol 2008;49:217–22.
[23] Wu H, Wilkins LR, Ziats NP, Haaga JR, Exner AA. Real-time monitoring of radiofrequency ablation and postablation assessment: accuracy of contrast-enhanced US in experimental rat liver model. Radiology 2014;270:107–16.
[24] Ji Q, Xu Z, Liu G, Lin M, Kuang M, Lu M. Preinjected fluids do not benefit microwave ablation as those in radiofrequency ablation. Acad Radiol 2011;18:1151–8.
[25] Tanaka T, Westphal S, Isfort P, Braunschweig T, Penzkofer T, Bruners P, et al. Microwave ablation compared with radiofrequency ablation for breast tissue in an ex vivo bovine udder model. Cardiovasc Intervent Radiol 2012;35:914–20.
[26] Yoshinaga Y, Enomoto Y, Fujimitsu R, Shimakura M, Nabeshima K, Iwasaki A. Image and pathological changes after radiofrequency ablation of invasive breast cancer: a pilot study of nonsurgical therapy of early breast cancer. World J Surg 2013;37:356–63.
[27] Boetes C, Mus RD, Holland R, Barentsz JO, Strijk SP, Wobbes T, et al. Breast tumors: comparative accuracy of MR imaging relative to mammography and US for demonstrating extent. Radiology 1995;197:743–7.